Experiments on Penetration Response of a Cylindrical Object into Rock Under Impact Loads

Ömer AYDAN[1*] and Shinya KODATE[2]

[1*]Member of JSCE, Professor, Dept. of Civil Eng., University of the Ryukyus
(Senbaru 1, Nishihara-cho, Okinawa 903-0213, Japan)
[2]Member of JSCE, Chuden Engineering Consultants
(2-3-30, Desio, Minami-ku, Hiroshima, 734-8510, Japan)
E-mail:aydan@tec.u-ryukyu.ac.jp

The authors developed a practical drop-weight type testing equipment and utilized for different purposes. In this study, the authors have used this device to investigate the penetration response of cylindrical objects into rock under different impact velocities. The authors utilized paraffin as a frictionless elastic-perfectly plastic material and Oya tuff and Ryukyu limestone as brittle rocks for impact tests. The author reports the outcomes of experimental results and discusses their implications in rock mechanics and rock engineering. Experiments showed that penetration depth and normalized tip stresses are proportional to momentum imposed on samples and relations developed are in good agreement with experimental results.

Key Words : *penetration,parafin, tuff, limestone, impant, cylindrical objects, shock device.*

1. INTRODUCTION

The penetration response of cylindrical objects into rock may be of great interest in some certain fields such as impact type excavation, demolition of structures and impact of meteorites (Fig. 1). For this purpose, split Hopkinson pressure bar (SHPB), drop-weight shock device are commonly used.

The authors developed a practical drop-weight type testing equipment and utilized for different purposes[1,2,3,4,5,6,7)]. In this study, this device was used to investigate the penetration response of cylindrical objects into rock under different impact velocities. Paraffin was selected as a frictionless elastic-perfectly plastic material while Oya tuff and Ryukyu limestone were chosen as brittle rocks. The drop height was varied in order to investigate the effect of impact velocity as well as the momentum imposed on samples. During experiments, the load and accelerations induced by shock loads are simultaneously measured and the fracturing state was recorded through high-speed video-cameras. The outcomes of experimental results and discusses their implications in rock mechanics and rock engineering.

Fig. 1. Some examples impact induced damage.

2. SHOCK DEVICE AND THEORETICAL CONSIDERATIONS

(1) Shock Device

A new experimental apparatus was developed to investigate the behaviour of rocks under shock waves as shown in Fig. 2. The device equipped with load cell, non-contact laser transducers, accelerometer up to 500G. The non-contact type laser displacement transducers measure the displacement of the loading platen. The load cell is capable of measuring much higher dynamic loads. The displacement of the loading platen is allowed to move downward up-to 20 mm in order to prevent the total destruction of samples upon failure. The cylindrical weight (5, 10 and 15 kgf) can be dropped from different heights up to 500 mm with an interval of 50 mm. The device may be fundamentally categorized as the drop-weight apparatus and it is possible to evaluate the mechanical behaviour and characteristics of rocks subjected to shock waves during pre-failure as well as post-failure stages. Some additional monitoring is done using infra-red camera and high-speed video camera.

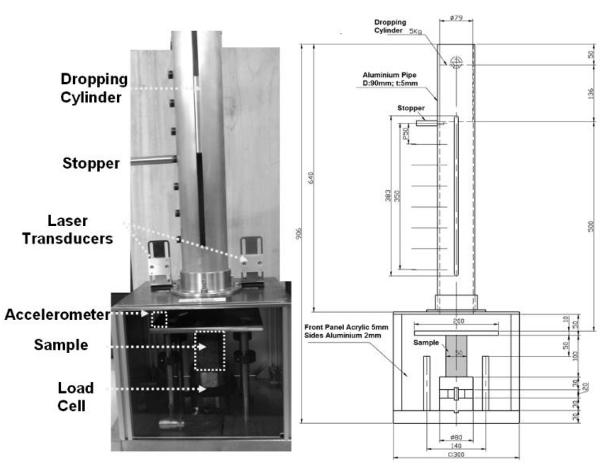

Fig. 2. A view and a schematic drawing of the testing device.

(2) Theoretical Considerations

The maximum nominal velocity at the time of impact on samples can be computed from the following formula:

$$V_{\max} = \sqrt{2gH_d} \tag{1}$$

where g is gravitational acceleration and H_d is drop height. In this study, we also define maximum nominal strain rate by dividing the maximum nominal impact velocity by the sample height for uniaxial testing condition as given below:

$$\dot{\varepsilon}_{\max} = \frac{V_{\max}}{L} \tag{2}$$

Maximum acceleration is obtained from the acceleration response during the experiment. It is expected that the maximum acceleration increases with the increase of strength of rock samples. On the basis of theoretical definition of momentum, the theoretical relation for momentum (P) applied to a sample may be written in the following form:

$$P = W\sqrt{\frac{2H_d}{g}} \quad \text{or} \quad P = W\frac{V_{\max}}{g} \tag{3}$$

Where W is the weight given in *kgf* or *N*. The unit utilized in processing experimental results is $N \cdot s$.

3. STATIC TESTING DEVICE

A static testing device named OA20KN was utilized for evaluating the penetration-load response under static condition as shown in Fig. 3. The device is displacement-controlled and its loading capacity is 20 kN.. The displacement rate utilized during static tests was 0.1 mm/s .

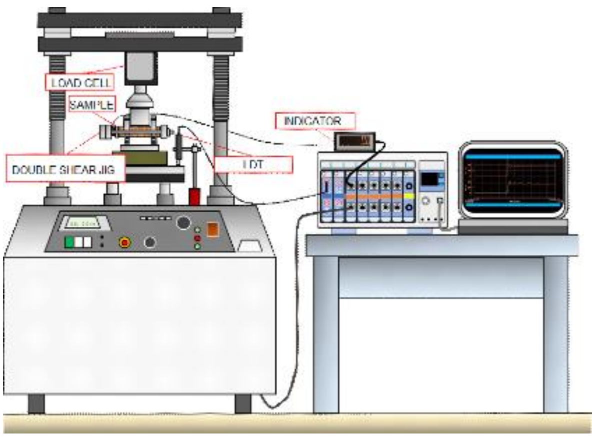

Fig. 3. Static testing devices OA20KN[8)]

4. MATERIALS AND IMPACT OBJECT

Paraffin, Oya tuff and Ryukyu limestone were used in experiments and impact device was hardened steel.. Fig. 4 shows views of samples tested under shock loads. In addition, some static tests were carried out to compare the difference in deformation responses and resistances under shock and static conditions.

Fig. 4. Views of samples tested.

(1) Paraffin

Paraffin was the pioneering material for researchers to study the fracturing and formulating elasto-plasticity and elasto-visco-plasticity. In non-linear regime, its behavior is perfectly plastic and its friction angle is known to be nil. This material was chosen to investigate the effects of various parameters such as drop height and weight so that the effect of momentum imposed on impact objects. Furthermore, the material is commercially available with very low cost. The diameter of the samples was 50 mm while its height was 50 mm Table 1 gives the physico-mechanical properties of paraffin samples tested.

Table 1. Physico-mechanical properties of paraffin.

γ (kN/m^3)	V_p (km/s)	V_s (km/s)	UCS (MPa)
0.89-0.9	1.86-2.19	0.79-1.05	1.71

(2) Rock Samples

Ryukyu limestone is widely distributed in Ryukyu Archipelago. Depending upon the formation process, it is fundamentally divided into coral, sandy and conglomeratic limestone. Samples of sandy (locally known as Awaishi) Ryukyu limestone, Oya tuff were prepared. The nominal size of samples were 50x50x50 mm. Table 2 summarizes mechanical properties of rck samples.

(3) Impact Object

The impact object has a shape of cylinder with a diameter of 10 mm and height of 35 mm. It is made of hardened steel.

Table 2. Physico-mechanical Properties (static)

Rock	γ kN/m^3	V_p km/s	V_s km/s	σ_{tBR} MPa	UCS MPa
Awaishi	22.4	4.43	2.49	3.4	28.1
Oya tuff	16.6	1.87	1.15	0.5-1.0	4.7-11.2

5. EXPERIMENTS ON PARAFFIN

Dynamic impact tests were carried out by varying drop height from 200 mm to 350 mm while keeping the weight of drop cyclinder as 5 kgf (49.1 N). Fig. 5 shows views of the samples tested under static and dynamic conditions. The plastic zone in the vicinity of the impact object is whitish for the drop height of 200 mm while radial tensile fractures (angle between fractures is 120 degrees) developed for the drop height of 350 mm in addition to whitish plastic zone.

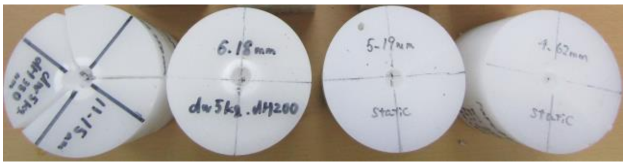

Fig. 5. Views of samples tested under static and dynamic loading conditions.

Fig. 6 shows the time-nominal tip pressure response for the drop heights of 200 and 350 mm. of the impact object. Nominal tip pressure is defined the ratio of dynamic force over the tip area of the cylindrical impact object. Fig. 7 shows the penetration versus nominal tip pressure response under static condition (loading velocity 0.1 mm/min). When both figures are compared, the dynamic resistance is more than 3 times than that under static condition.

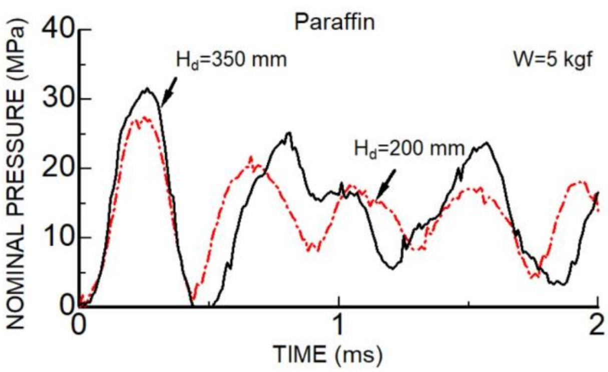

Fig. 6. Time vs nominal tip pressure response for different drop height under a drop weight of 5 kgf.

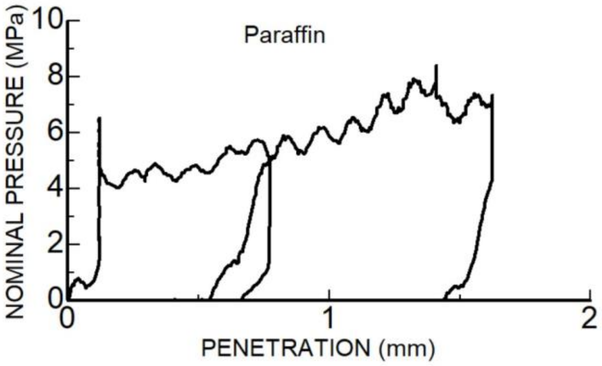

Fig. 7. Penetration vs nominal tip pressure response under static condition.

6. EXPERIMENTS ON ROCKS

(1) Experiments on Oya Tuff

Dynamic impact tests were carried out by varying drop height from 200 mm to 500 mm while keeping the weight of drop cyclinder as 10 kgf (98.1 N). Fig. 8 shows views of the samples tested under static and dynamic conditions. The plastic zones in the vicinity of the impact object appear as holes. In addition, radial fractures developed in dynamic and static tests. Fig. 9 shows the time-nominal tip pressure response for the drop heights of 200, 350 and 500 mm. Despite the variation of drop heights, the overall resistance remains almost constant. Fig. 10 shows the penetration versus nominal tip pressure response under static condition (loading velocity 0.1 mm/min). When both figures are compared, the dynamic resistance is more than 1.79 times than that under static condition.

Fig. 8. Views of samples tested under static and dynamic loading conditions.

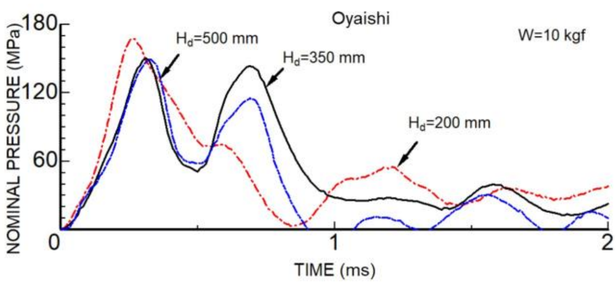

Fig. 9. Time versus nominal tip pressure response for different drop height under a drop weight of 10 kgf.

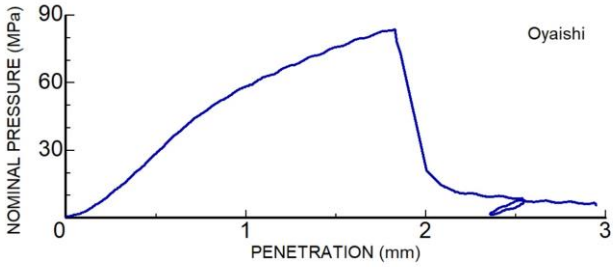

Fig. 10. Penetration versus nominal tip pressure response under static condition.

(2) Experiments on Awaishi

Dynamic impact tests were carried out by varying drop height from 200 mm to 350 mm while keeping the weight of drop cyclinder as 10 kgf (98.1 N). Fig. 11 shows views of the samples tested under static and dynamic conditions. The plastic zones in the vicinity of the impact object appear as holes. In addition, radial fractures developed in dynamic and static tests. Fig. 12 shows the time-nominal tip pressure response for the drop heights of 200 and 350 mm. Despite the variation of drop heights, the overall resistance remains almost constant. Fig. 13 shows the penetration versus nominal tip pressure response under static condition (loading velocity 0.1 mm/min). When both figures are compared, the dynamic resistance is more than 3 times than that under static condition..

(a) Dynamic

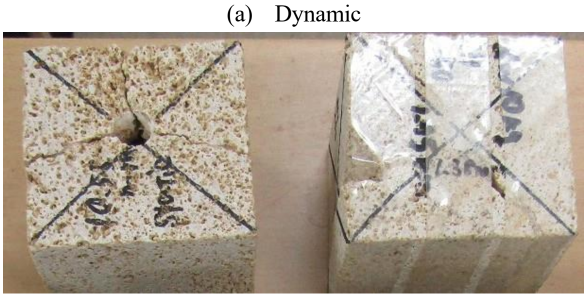

(b) Static

Fig. 11. Views of samples tested under static and dynamic loading conditions.

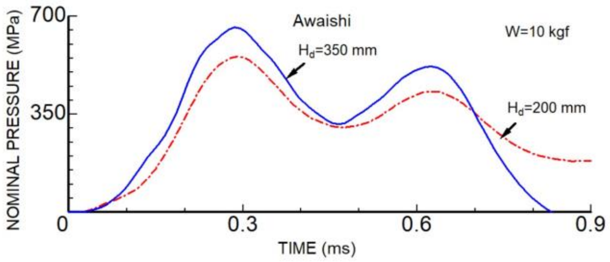

Fig. 12. Time versus nominal tip pressure response for different drop height under a drop weight of 10 kgf.

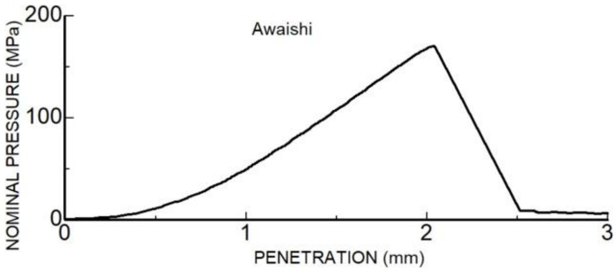

Fig. 13. Penetration versus nominal tip pressure response under static condition.

7. DISCUSSIONS

(1) Effect of Momentum

As noted from the experimental set-up, the height and weight of the drop object are the most important parameters on the amplitude of the imposed impact load. With this mind, the ratio of measured dynamic static tip pressures obtained from the experimental results are plotted in Fig. 14 as a function of the momentum theoretically defined by Eq. (3). The experimental results differ depending upon the material type and they are fitted to a linear function.

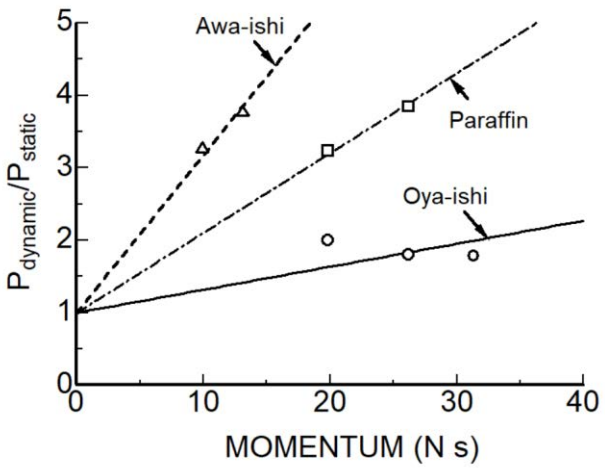

Fig. 14. Momentum versus the ratio of dynamic tip pressure over the static tip pressure.

(2) Penetration and Damage

The penetration depth and damage around the impact object differ depending upon the height and weight of the drop object as well as the characteristics of the materials. Fig. 15 shows the penetration strain defined as the ratio of penetration (δ) over the diameter of the cylindrical impact object as a function of momentum given by Eq. (3). The experimental results are fitted to the following function

$$\frac{\delta}{D} = aP^2 \tag{4}$$

Where a is empirical constant.

As noted from Fig. 15, the empirical relation given by Eq. (4) presents a good fit to the experimental results. Fig. 16 shows the plastic zone under static and dynamic conditions. The plastic zone development is co-centric and expands outward depending upon the momentum imposed on the cylindrical impact object. Fig. 17 shows the plastic zone development in the vertical cross-section. As noted from the figure, a semi-spherical plastic zone occurs beneath the tip of the cylindirical impact object and propagates as the amount of the penetration increases. However, radial fractures develop as the penetration depth increases irrespective of material type.

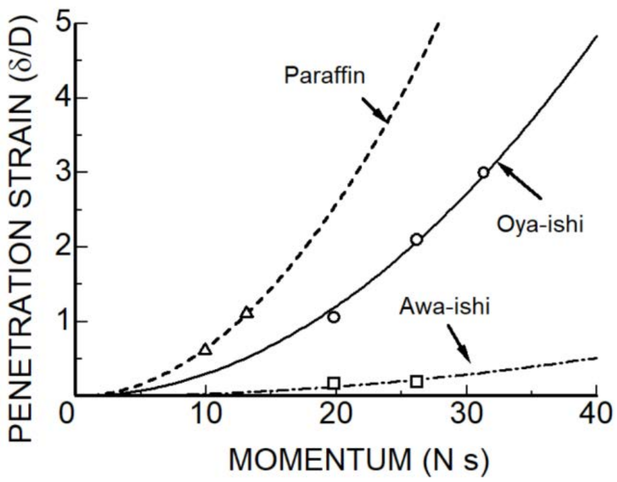

Fig. 15. Experimental results for momentum versus penetrations strain.

(3) Effect of Brittleness

As pointed out previously, paraffin is a perfectly plastic ductile material while Oyaishi and Awaishi are brittle materials. Figures 5, 8 and 11 show the post-test views of samples while Figs. 16 and 17 show close-up views of plastic zones. Fundamentally, plastic zone development are similar for both ductile and brittle materials. Nevertheless, radial fractures due to tensile stresses occur and they become dominant after a certain amount of penetration.

Paraffin Oyaishi Awaishi

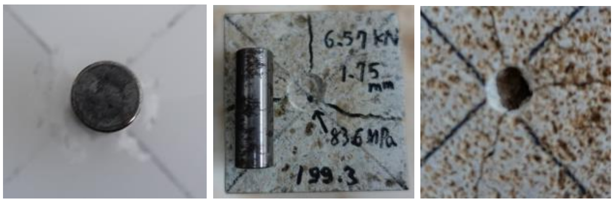

(a) static

(b) dynamic

Fig. 16. Plastic zones under static and dynamic conditions.

Paraffin Oyaishi Awaishi

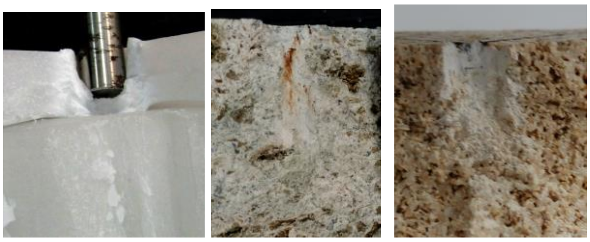

Fig. 17. Plastic zones in vertical cross-sections.

8. CONCLUSIONS

A practical drop-weight type testing equipment was utilized to investigate the penetration response of cylindrical objects into rock under different impact velocities. Paraffin was used as a frictionless elastic-perfectly plastic material while Oya tuff and Ryukyu limestone are used as brittle rocks. Experimental results indicated that momentum related to the height and weight of the impact object and defined by Eq. (3) is an important parameter to explain experimental results. The dynamic tip pressure is a linear function of the momentum while the pentrtion strain defined as the ratio of penetration over the diameter of the impact object obeys the power function.

ACKNOWLEDGMENT

We gratefully acknowledge Chuden Engineering Consultants (Hiroshima) for financial support for this experimental study.

REFERENCES

1) Aydan, Ö., Ito, T., Tokashiki, N., and, Kodate, S.: Shock Tests and Some considerations. *Proceedings of ISRM 14th International Congress of Rock Mechanics* – Foz do Iguassu, Brazil, 1085-1092, 2019.
2) Kodate, S., Tomiyama, J., Suda, Y., Horiuchi, K. and Aydan, Ö.: Mechanical behaviour and characteristics of rocks subjected to shock loads. *Proceedings of 2019 Rock Dynamics Summit in Okinawa*, Japan, ISRM (Editors: Aydan, Ö., Ito, T., Seiki T., Kamemura, K., Iwata, N.), 646-651, 2019.
3) Kodate, S.. A Fundamental Study on the Dynamic Deformation and Fracture Characteristics of Rocks under Shock Loads. Master Thesis, 140p, *University of the Ryukyus*, Okinawa, Japan 2021
4) Kodate, J. Tomiyama, Y. Suda, K. Horiuchi, Ö. Aydan.. Mechanical behaviour and characteristics of rocks subjected to shock loads. *Proceedings of 2019 Rock Dynamics Summit in Okinawa*, Japan, ISRM (Editors: Aydan, Ö., Ito, T., Seiki T., Kamemura, K., Iwata, N.), 646-651, 2019.
5) Aydan, Ö., Kodate, S., Tomiyama, J., Suda, Y. and Iwata, N.. Experiments on bonding characteristics of rock-bolts/rockanchors under shock loads. *The 55th US Rock Mechanics/Geomechanics Symposium*, Texas, Paper No ARMA 21-1632, 8p, 2021.
6) Aydan, Ö., Kodate, S. and Iwata, N.. A New Double Shearing Testing Equipment for the Shear Behaviour of Rocks and Discontinuities under Static and Shock Loads. E*uropean Rock Mechanics Symposium, EUROCK2021*, Torino, 8p, 2021.
7) Aydan, Ö., Kodate, S. and Iwata, N.. The effect of aspect ratio of rock samples on the dynamic characteristics of rocks under shock loads. *The 11^{th} Asian Rock Mechanics Symposium (ARMS11),* Beijing, Paper No. F0154, 8p., 2021
8) Aydan, Ö.., Daido, M., Tano, H., Nakama, S. and Matsui, H. The failure mechanism of around horizontal boreholes excavated in sedimentary rock. 50th US Rock mechanics Symposium, Paper No. 06-130 (on CD)., 2006.